CHAPTER II

DATA

2.1 Introduction

In this study the teleseismic earthquakes recorded by TOR and SVEKALAPKO (Fig. 2.1), two of the largest deployments of temporary seismic networks in Europe, and the German Regional Seismic Network (GRSN) have been utilized (Fig. 2.1). Descriptions of each database which include statistical aspects of the data set are presented in designated sections. In the end, the quality of signal in some representative stations is briefly discussed.

2.2 TOR

The TOR temporary seismic network consisted of 33 broadband (Table B.1, Appendix B) and 108 short−period stations (Table B.2, Appendix B) and was operational during September 1996 – March 1997 (*Gregersen et al. 1999*). It has been an initiative of the international, interdisciplinary TOR (Teleseismic Tomography **TOR**nquist, *Gregersen et al. 1999)* project that aimed at better understanding of the structure and formation of part of the Trans−European Suture Zone (TESZ) in northern Europe, called Tornquist Zone. It followed a pilot study which involved the deployment of 14 braodband stations along a 100 km long profile across the Tornquist Zone in Denmark and Sweden in 1993−1994 (*Kind et al. 1997*). The main TOR profile stretched along a strip of 900 km long and 100 km wide from Harz mountains, Germany in the south, over Denmark to Sweden in the north by crossing the Elbe Line, and the Tornquist Zone (Fig. 2.1). The subsidiary profile which extended 400 km over the North German Basin coincided with the site of an active seismic survey, DEKORP−BASIN '96 (*DEKORP−BASIN Research Group 1999*) and thus provided the unique opportunity for comparing the results of active and passive seismic surveys (*Gossler et al. 1999*).

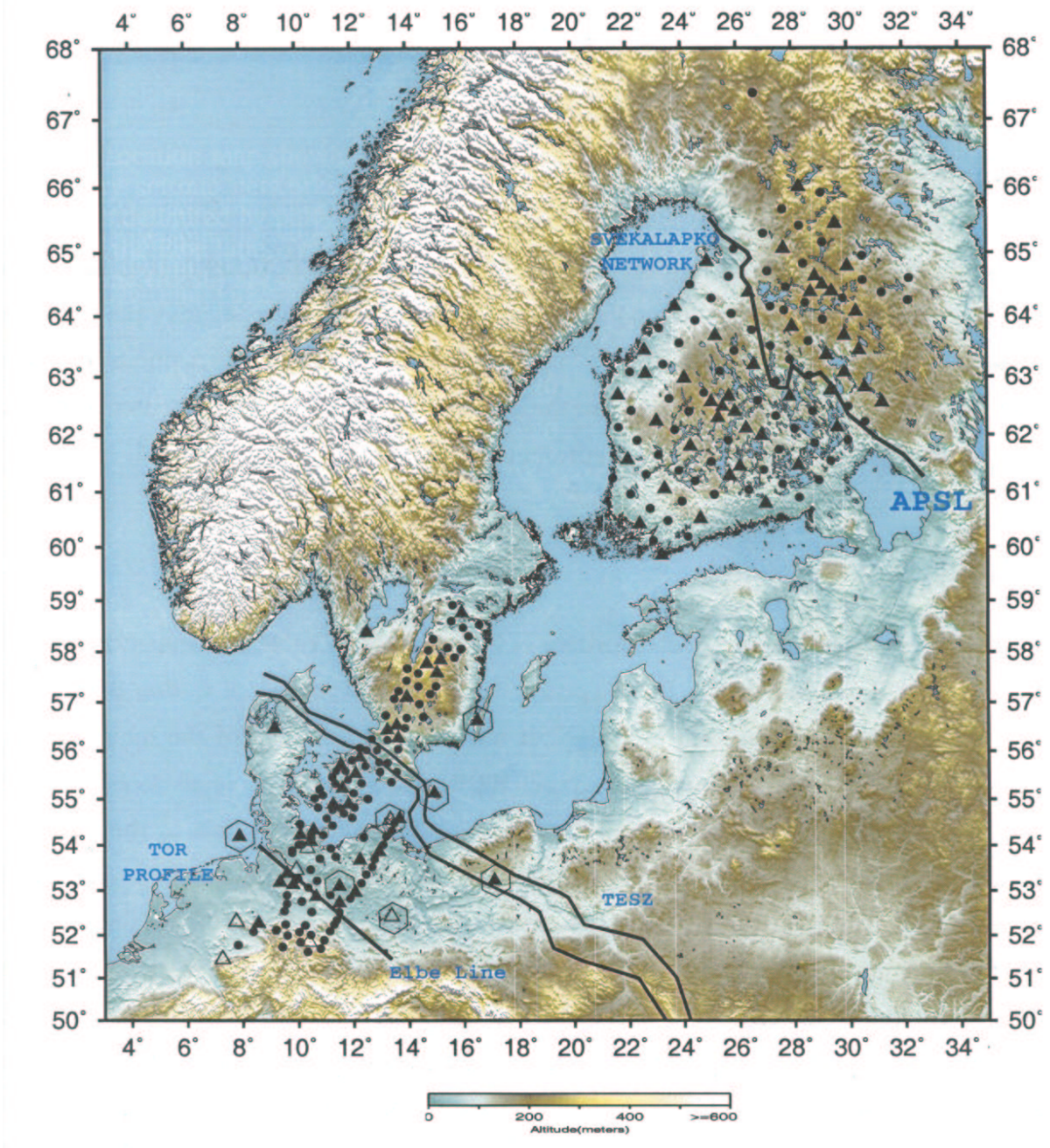

Fig. 2.1 Location map showing the distribution of the stations of the TOR and SVEKALAPKO temporary seismic networks and those stations of GRSN (hollow triangles) and GEOFON (triangles delimited by polygons) networks whose data have been used in this study. Labeled traces of the Elbe Line, Trans−European Suture Zone (TESZ) and the Archean−Proterozoic Suture Line (APSL) are also to be seen.

A total number of 24 teleseismic earthquakes (Table A.1, Appendix A) in the epicentral distance range of 30°−90° with threshold magnitude of 5.9 have been used in this study (Fig. 2.2). Only one event with M=5.6 which proved to be of good quality was included in the data set. Figs. 2.2−2.5 show some characteristics of this database.

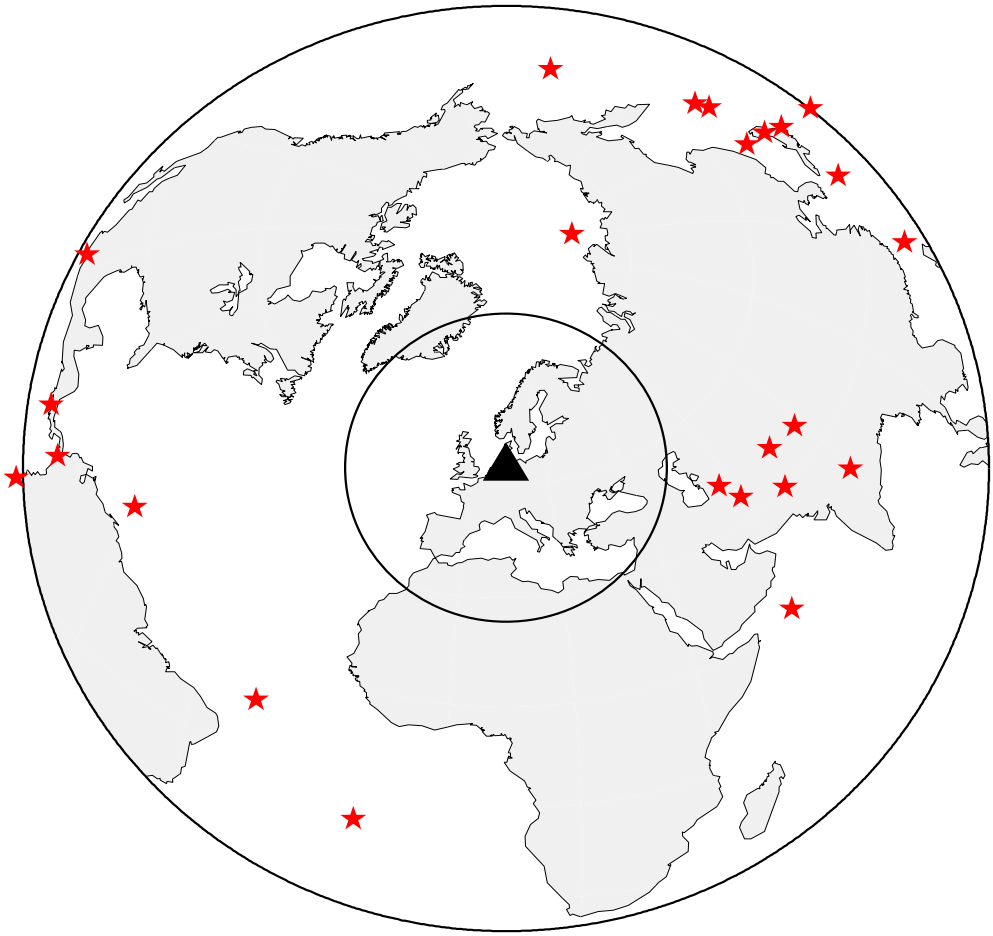

Fig 2.2 Distribution of 24 teleseismic earthquakes (Table A.1, Appendix A) as recorded by TOR seismic network during its operation from August 1996 through May 1997.

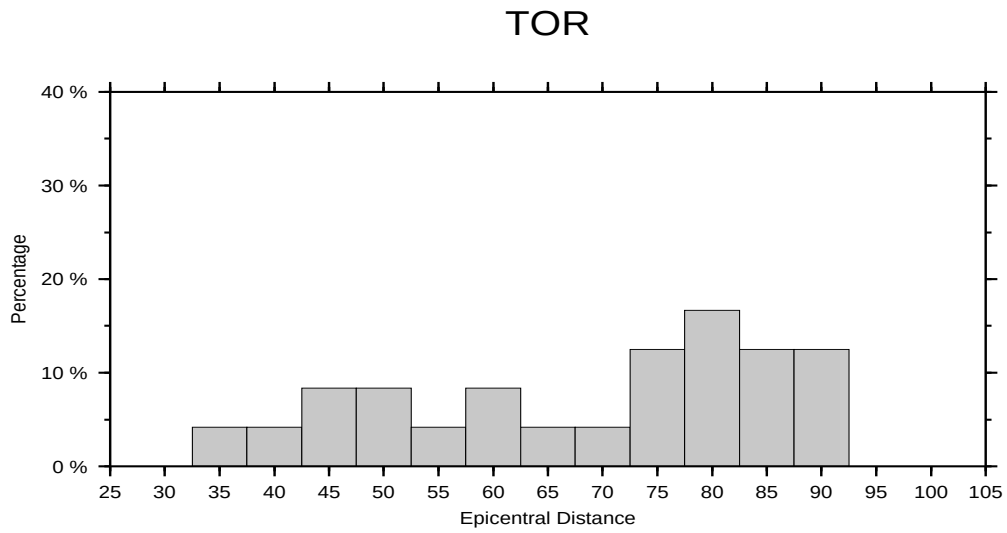

Fig. 2.3 Histogram showing the distribution of recorded events by TOR network (Table A.1, Appendix A) in terms of their epicentral distances from the network.

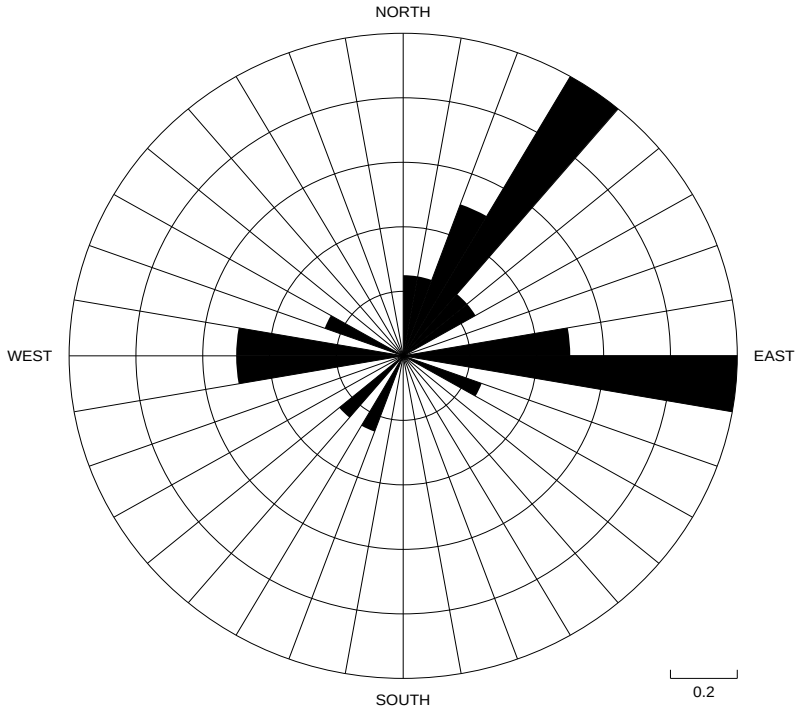

Fig. 2.4 Rose diagram showing the azimuthal distribution (normalized) of events (Table A.1, Appendix A) recorded by the TOR network.

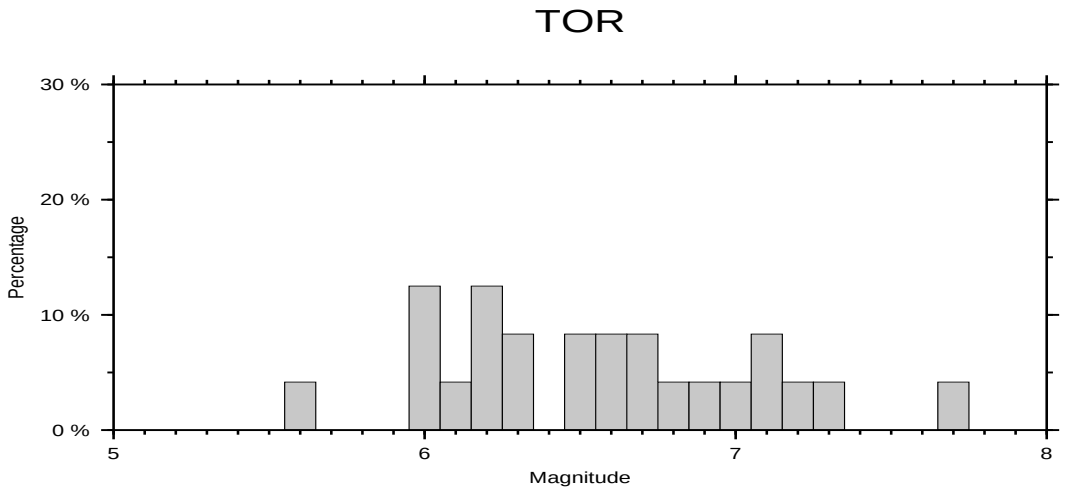

Fig. 2.5 Histogram showing the percentage distribution of events (Table A.1, Appendix A) in terms of their magnitude as recorded by TOR network.

2.3 GRSN

The German Regional Seismic Network (GRSN) is a network of broadband stations in Germany that is operational since 1991−1993. In order to improve on the azimuthal distribution of the TOR data, 123 teleseismic earthquakes (Table A.2, Appendix A) with epicentral distances of 30°−95°, signal to noise ratio greater than 2, and threshold magnitude of 6.0, which were recorded by 7 stations of GRSN stations (Table B.3, Appendix B) during 1991−1998 have been included in TOR data. Figs 2.6−2.9 show some characteristics of this database..

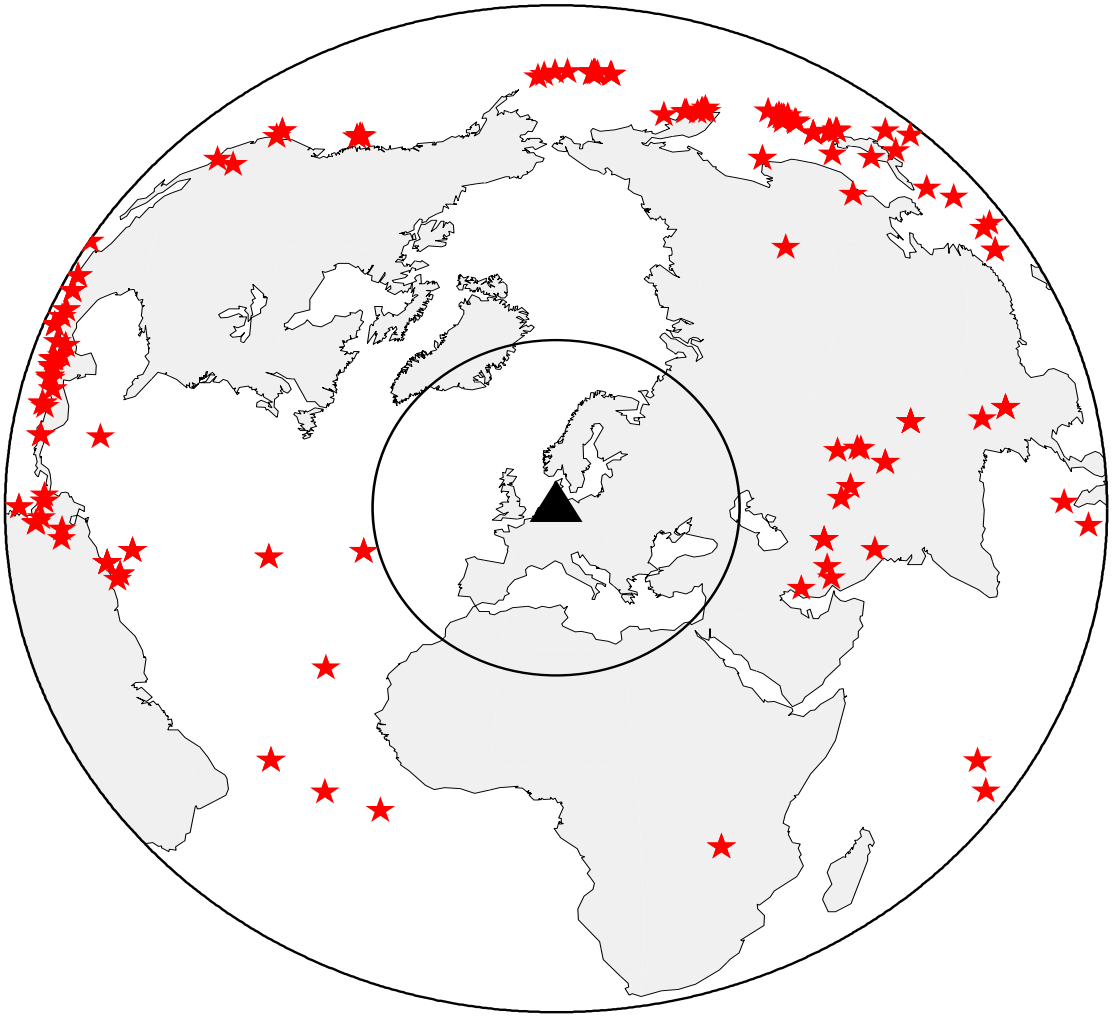

Fig. 2.6 Distribution of 123 teleseismic earthquakes (Table A.2, Appendix A) with SNR greater than 2 as recorded by GRSN during 1992−1999 and used in this study.

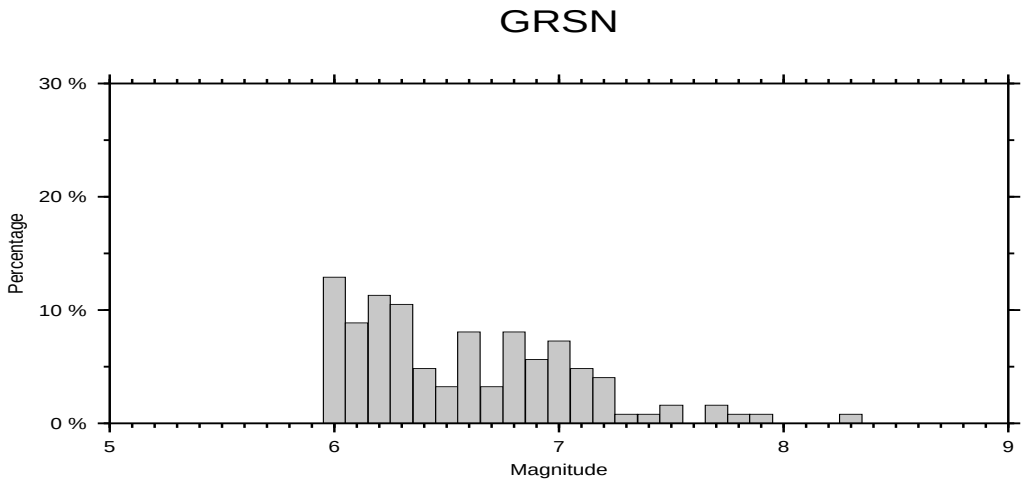

Fig. 2.7 Histogram showing the percentage distribution of events (Table A.2, Appendix A) in terms of their magnitude as recorded by GRSN.

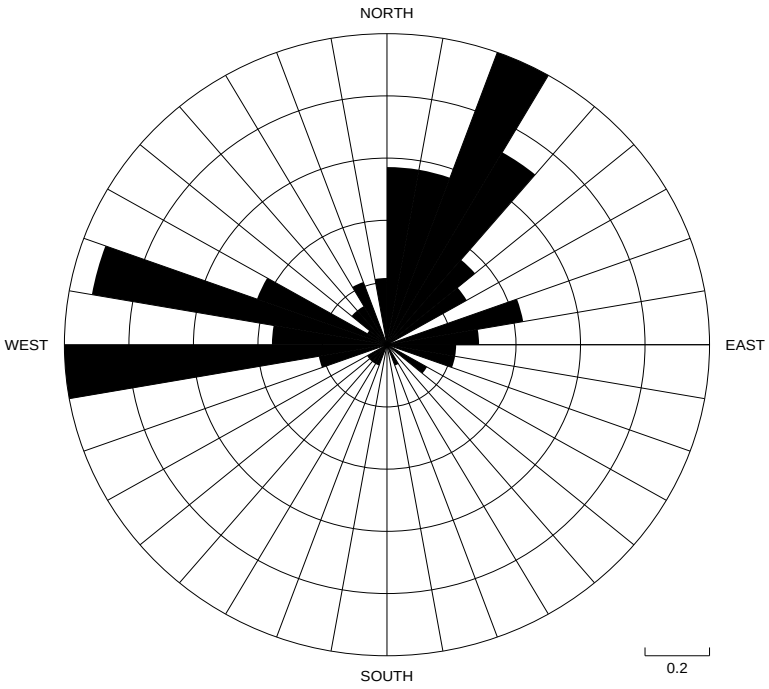

Fig. 2.8 Rose diagram showing the azimuthal distribution (normalized) of events (Table A.2, Appendix A) recorded by GRSN.

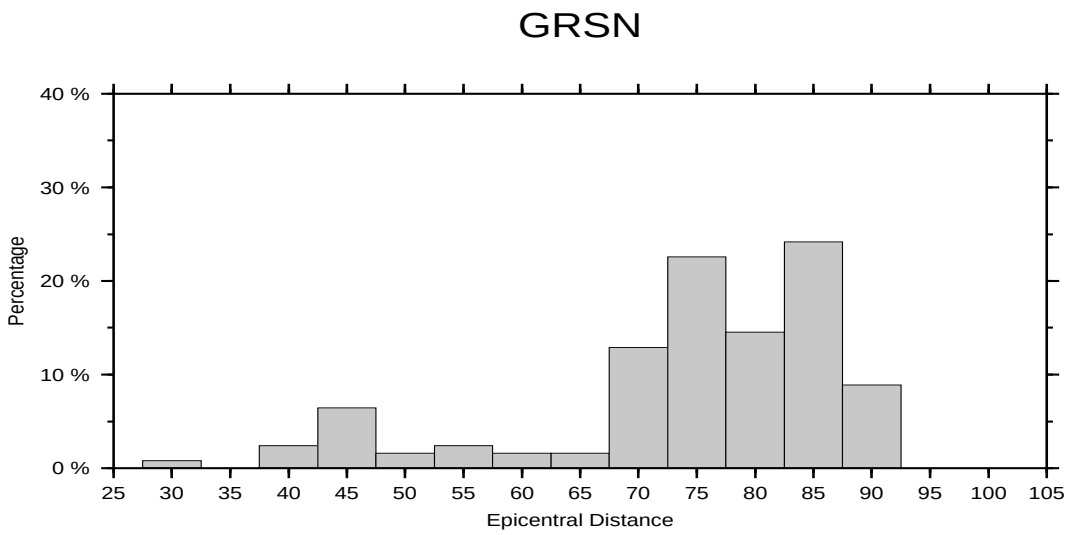

Fig. 2.9 Histogram showing the distribution of recorded events by GRSN (Table A.2, Appendix A) in terms of their epicentral distances from the network.

2.4 SVEKALAPKO

The SVEKALAPKO (**SV**ecofennian **KA**relian−**LA**pland−**KO**la Transect) seismic network has been a large deployment of stations over the Baltic Shield which was operational during August 1998 – April 1999 stretching from southern Finland to southwest Russia (Fig. 2.1) (*Bock et al. 2001*). It has been part of a multidisciplinary international project that aimed at unraveling the crust and lower lithosphere structure of the Baltic Shield (*Hjelt & Daly 1996*).

A total number of 85 teleseismic earthquakes (Table A.3, Appendix A) in the epicentral distance range of 30°−95° with threshold magnitude of 5.7 recorded by 46 broadband stations (Table B.6, Appendix B) and 77 short−period stations (Table B.7, Appendix B) have been utilized in this study (Fig. 2.1). Fig. 2.10−2.13 show some characteristics of this database.

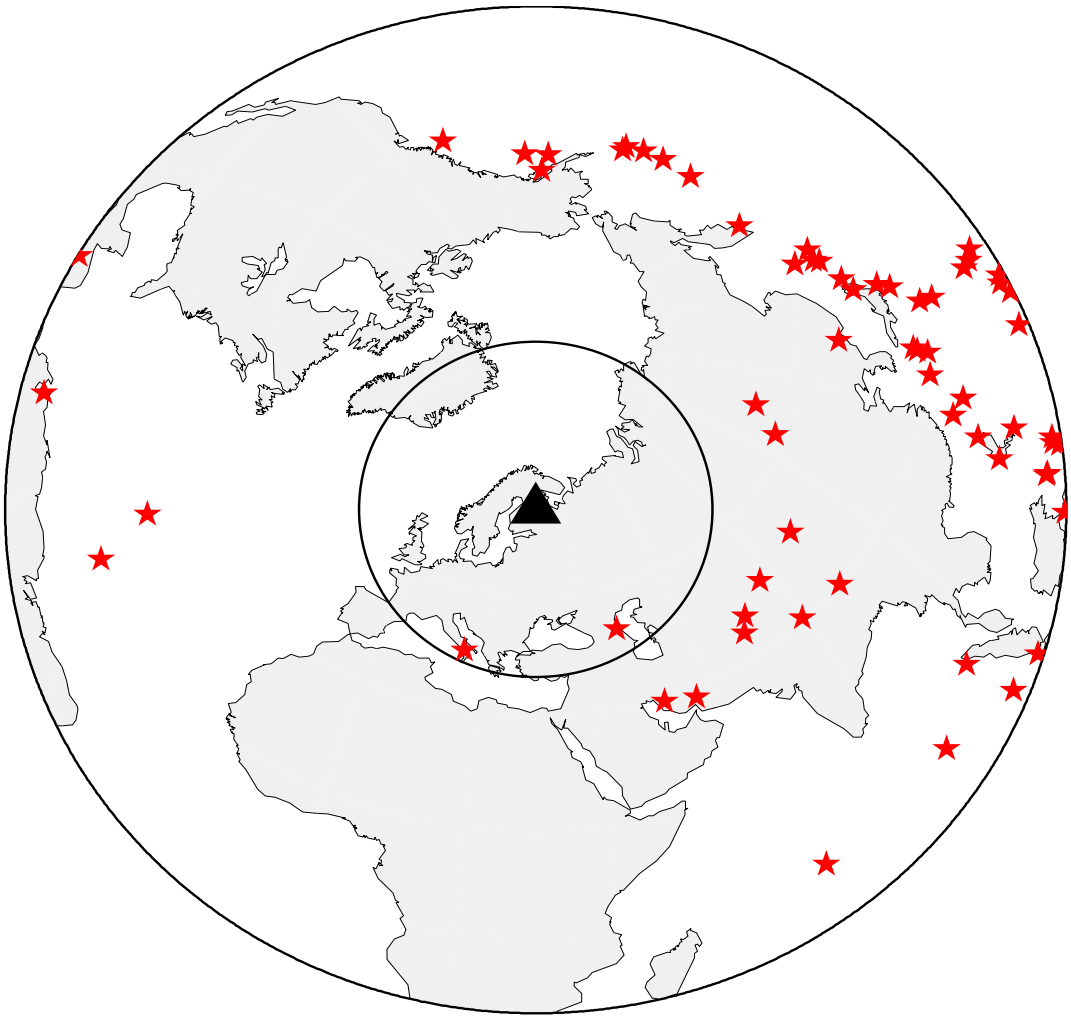

Fig. 2.10 Distribution of 123 teleseismic earthquakes (Table A.3, Appendix A) as recorded by SVEKALAPKO seismic network during its operation from August 1998 through May 1999.

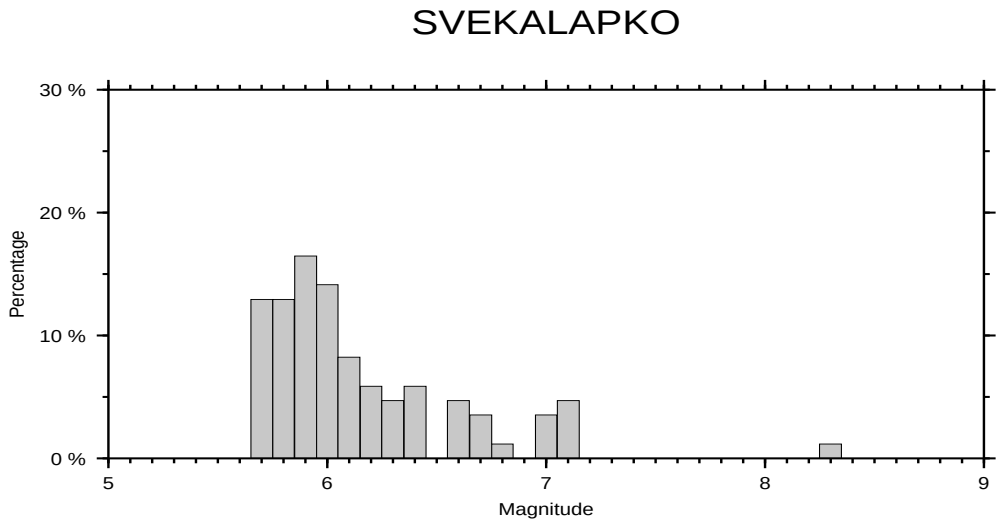

Fig. 2.11 Histogram showing the percentage distribution of recorded events (Table A.3, Appendix A) by SVEKALAPKO network in terms of their magnitudes.

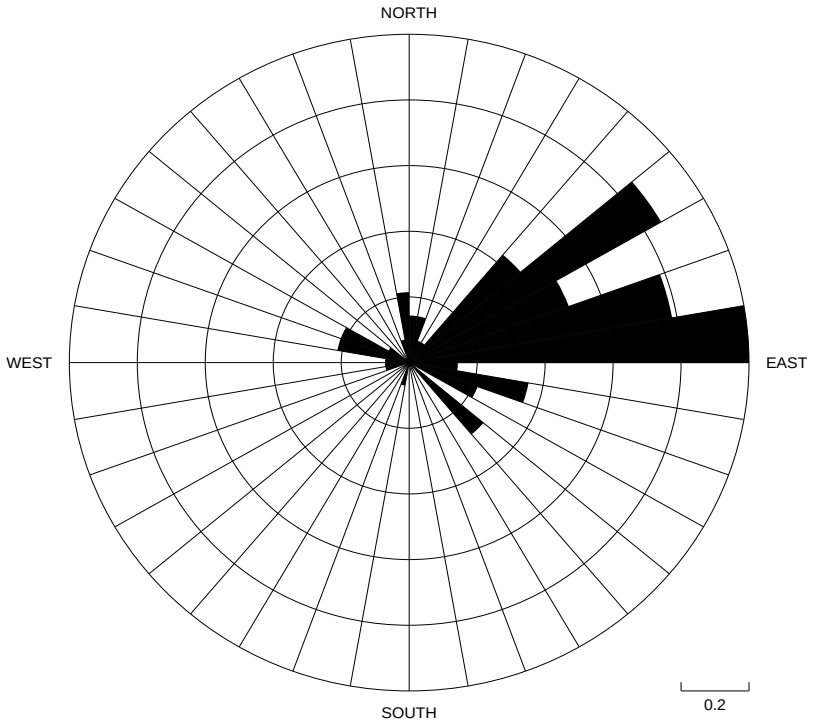

Fig. 2.12 Rose diagram showing the azimuthal distribution (normalized) of events (Table A.3, Appendix A) recorded by the SVEKALAPKO network.

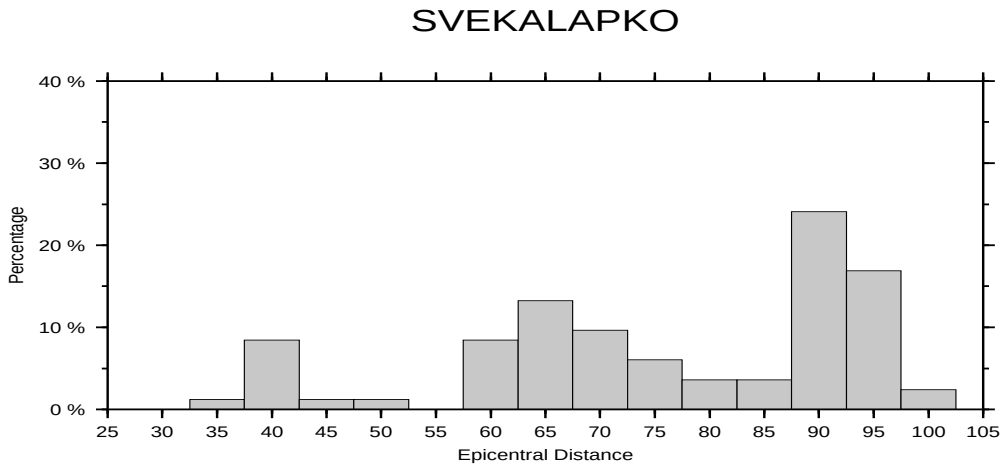

Fig. 2.13 Histogram showing the distribution of recorded events by SVEKALAPKO network (Table A.3, Appendix A) in terms of their epicentral distances from the network.

2.5 Signal quality

To show the quality of earthquake signals recorded at TOR, SVEKALAPKPO, and GRSN networks, amplitude spectra of P wave and preceding background noise for a few stations are shown in Fig. 2.14 to Fig. 2.19. The spectra have been calculated from the recorded seismograms (uncorrected for instrument effects) and show that for medium magnitude earthquakes ($M \cong 6$) the amplitude of recorded signals becomes close to background noise. Assuming that the background noise is white noise then constructive summation of receiver functions (stacking) can help to reduce noise amplitudes and thereby increases signal to noise ratio. Since the desired teleseismic P signals have frequencies lower than 1 Hz applying a lowpass filter of 1Hz can significantly reduce the high frequency noise without damaging the signal content significantly. The inherent lack of high frequency signal in teleseismic P coda, combined with additional removing of high frequency content through usually necessary lowpass filtering characterizes the spacial resolution of the receiver function technique.

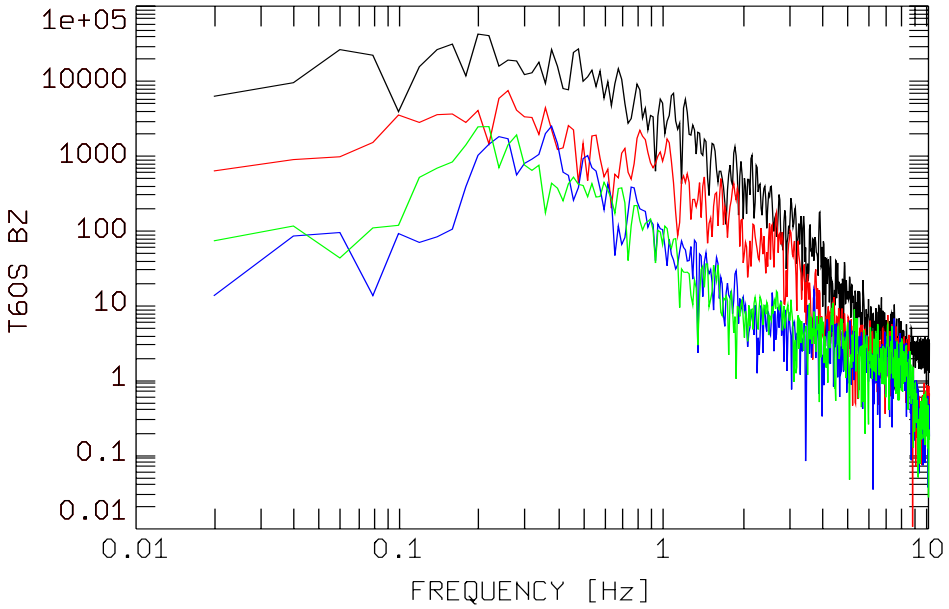

Fig. 2.14 Amplitude spectra of recorded P signals and the preceding noise at a broadband station of TOR network (T60S, table B.1, appendix B) for an M=7.7 event (event No. 22, Table A.1, Appendix A) depicted in red and green, respectively and for an M=6.1 event (event No. 9, Table A.1, Appendix A) depicted in black and blue, respectively.

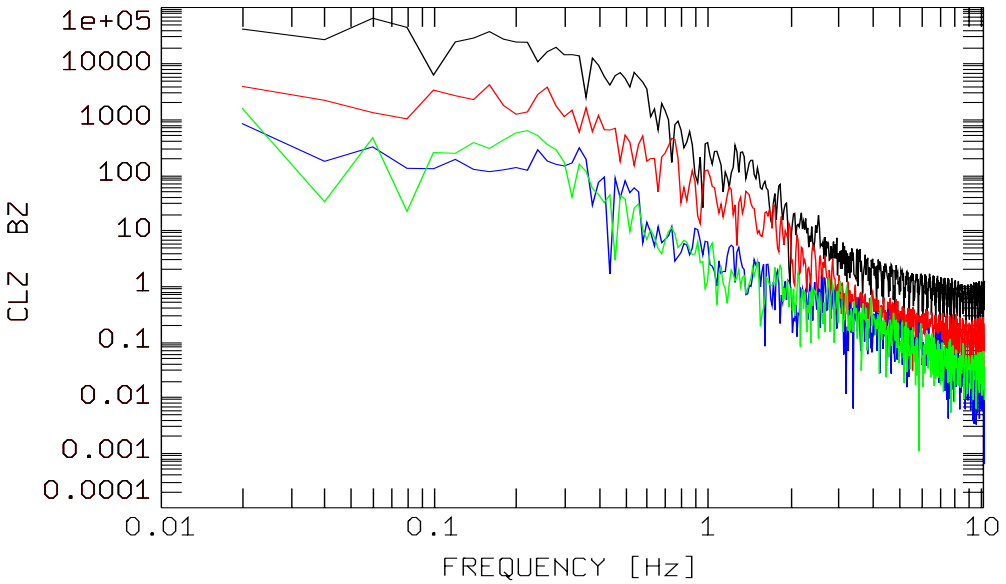

Fig. 2.15 Amplitude spectra (Z component) of recorded P signals and the preceding noise at a broadband station of GRSN network (CLZ, table B.3, appendix B) for an M=7.7 event (event No. 22, Table A.1, Appendix A) depicted in red and green, respectively and for an M=6.1 event (event No. 9, Table A.1, Appendix A) depicted in black and blue, respectively.

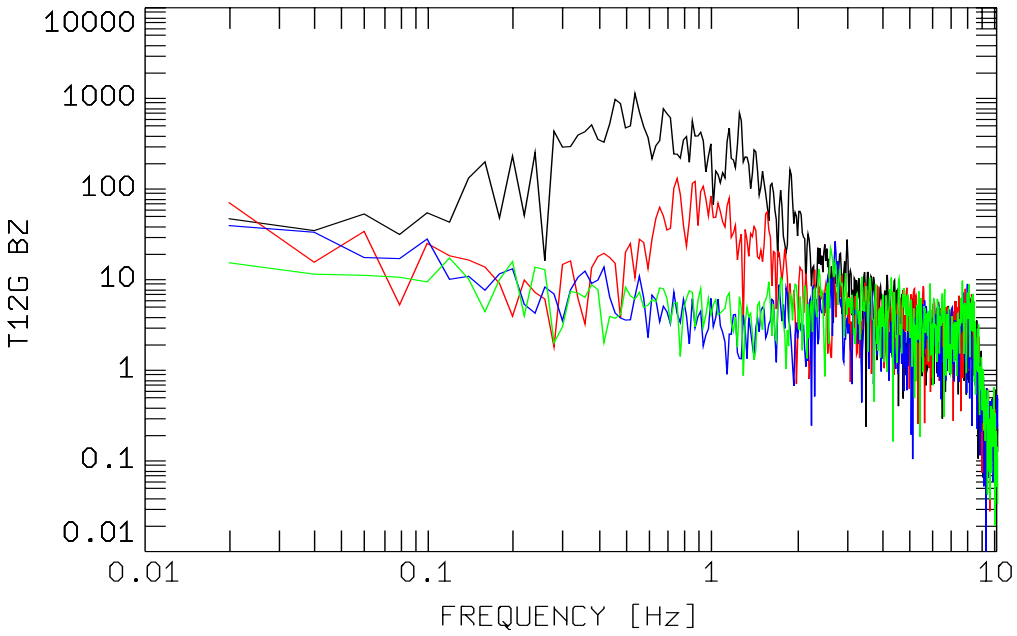

Fig. 2.16 Amplitude spectra (Z component) of recorded P signals and the preceding noise at a short−period station of TOR network (T12G, table B.2, Appendix B) for an M=7.7 event (event No. 22, Table A.1, Appendix A) depicted in red and green, respectively and for an M=6.1 event (event No. 9, Table A.1, Appendix A) depicted in black and blue, respectively.

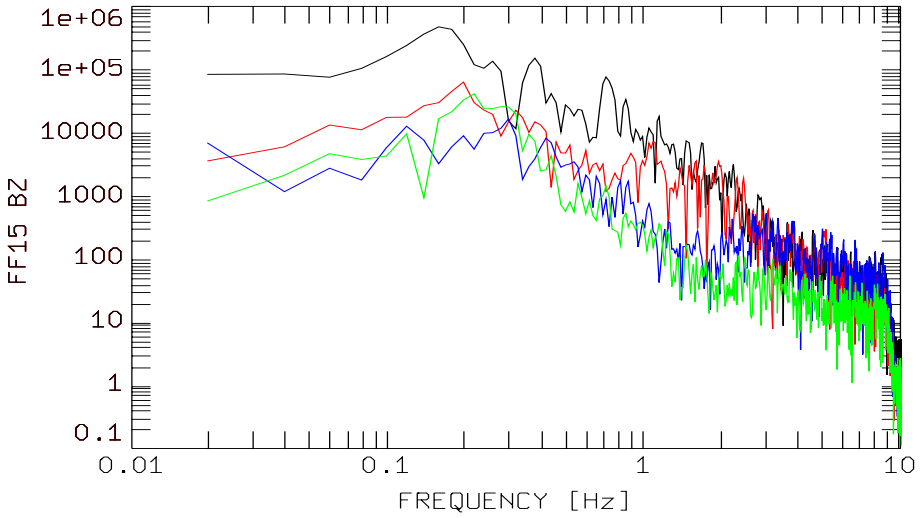

Fig. 2.17 Amplitude spectra (Z component) of recorded P signals and the preceding noise at a broadband station of SVEKALAPKO network (FF15, table B.6, appendix B) for an M=6.6 event (event No. 66, Table A.3, Appendix A) depicted in red and green, respectively and for an M=6.0 event (event No. 72, Table A.3, Appendix A) depicted in black and blue, respectively.

In order to show the importance of site selection in deployment of seismic stations spectra of recorded P wave and preceding background noise are shown in Fig. 2.16 and Fig. 2.17. In each figure the two stations have the same instrumentation and have recorded the same event. Thus the site effect on signal quality can be directly studied.

A point that deserves to be made here is the effect of the presence of kilometers of sedimentary layers on the frequency content of recorded seismograms. To the south of 56°N latitude across the North German Basin the presence of thick sedimentary layers covering the crystalline bed rocks leads to strong attenuation of high frequency content signals so that stations across SVEKALAPKO network show higher frequency content than stations in TOR project (specially south of the Tornquist Zone across the North German and Danish Basins). It will be shown later how this inherent difference in frequency content can influence the resolution.

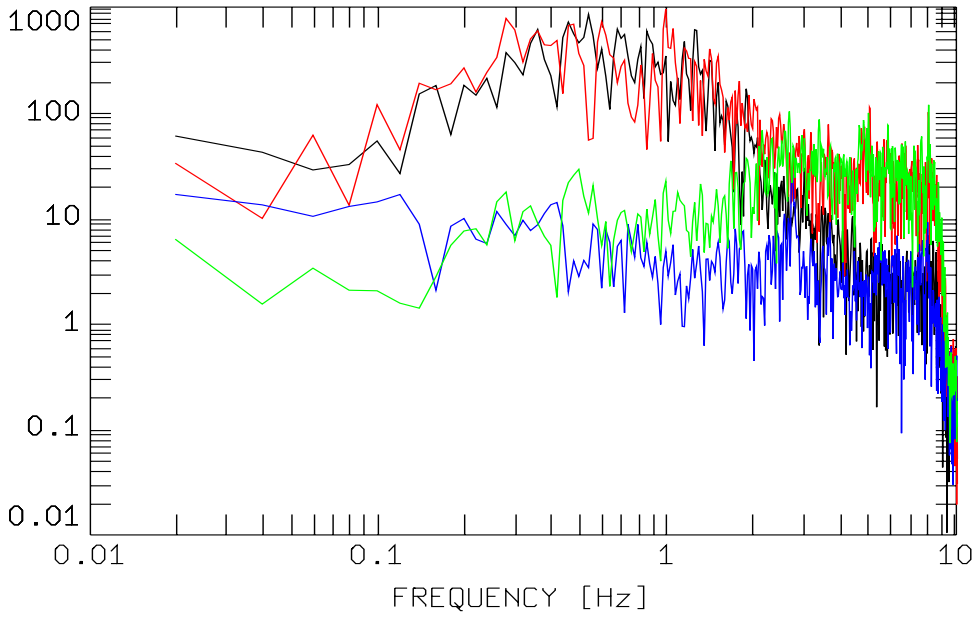

Fig. 2.18 Amplitude spectra (Z component) of P wave and the preceding background noise for an M=7.7 event (event No. 22 , Table A.1, Appendix A) recorded by station T12G (Table B.2, appendix B) depicted in black and blue, respectively and station T60G (Table B.2, Appendix B) depicted in red and green, respectively. Both stations are short period stations equipped with the same recording systems and therefore provide basis for comparing the site effect on signal quality.

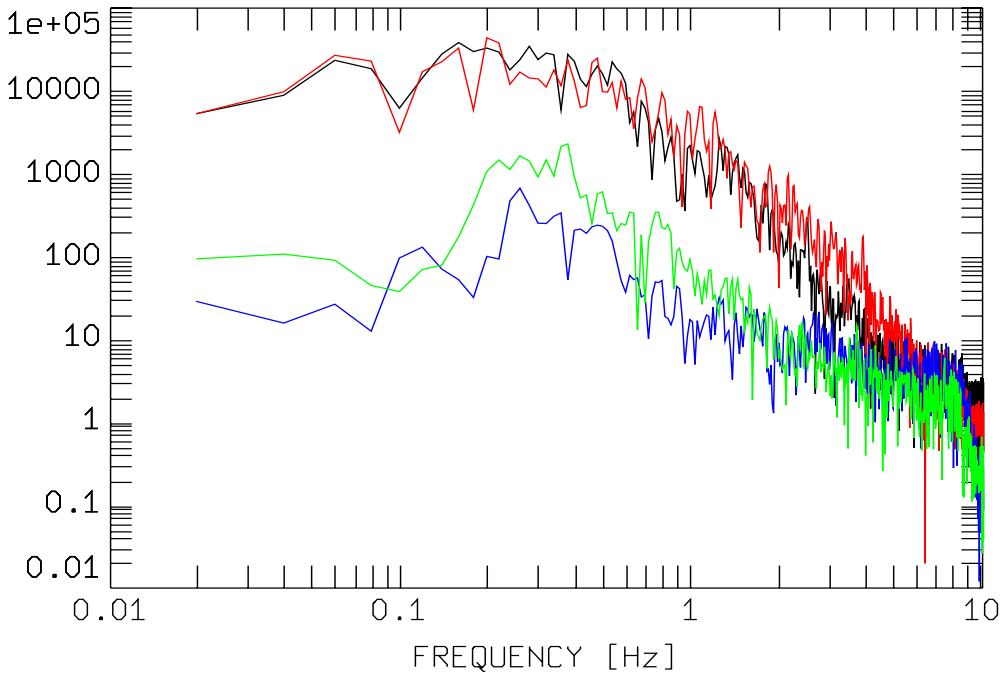

Fig. 2.19 Amplitude spectra (Z component) of P wave and the preceding noise for an M=7.7 event (event No. 22 , Table A.1, Appendix A) recorded by station CLZ (Table B.3, Appendix B) depicted in black and blue, respectively and station T60S (Table B.1, Appendix B) depicted in red and green, respectively. Both stations are broadband stations equipped with the same recording systems and therefore provide basis for comparing the site effect on signal quality.